Available online at www.CivileJournal.org

Civil Engineering Journal

Vol. 4, No. 11, November, 2018

Predicting Dynamic Capacity Curve of Elevated Water Tanks: A Pushover Procedure

Afshin Mellati [a*]

[a] *School of Civil and Environmental Engineering, University of New South Wales, Sydney, Australia.*

Received 13 September 2018; Accepted 04 November 2018

Abstract

Despite the importance of water tanks for water supplies and supporting the community resilience through the firefighting usages in catastrophic conditions, post-earthquake situations especially, a few studies have been done on seismic behavior of water tanks so far. The scope of this paper is to propose a new pushover procedure to evaluate seismic responses of elevated water tanks (EWT) supported on the concrete shaft in the form of dynamic capacity curves (i.e. base shear versus top displacement). In this regard, a series of shaft supported EWTs are simulated considering soil-structure and fluid-structure interactions. The shaft is modelled with frame elements and plastic hinges are assigned along the shaft to consider the material nonlinearity. The effect of soil-structure interaction and fluid-structure interaction are considered through the well-known Cone model and modified Housner model, respectively. At first, parametric studies have been conducted to investigate the effects of various essential parameters such as soil type, water level and tank capacity on seismic responses of EWTs using incremental dynamic analysis (i.e. nonlinear-time-history-analyses with varying intensities). Thereafter, pushover analyses as nonlinear static analyses are performed by variation of lateral load patterns. Finally, utilizing these results and comparing them with mean IDA curve, as an exact solution; a pushover procedure based on the most reliable lateral load patterns is proposed to predict the mean IDA curve of the EWTs supported on the concrete shaft. The obtained results demonstrate the accuracy of the proposed pushover procedure with errors limited to 30 % only in the changing stage from linear to nonlinear sections of the IDA curve.

Keywords: Elevated Water Tank; Soil-Structure Interaction; Fluid-Structure Interaction; Load Pattern; Incremental Dynamic Analysis (IDA); Pushover; Nonlinear Response History Analysis (NLRHA).

1. Introduction

Water tanks are used for drinking, firefighting, agriculture, and different industrial plants [1-4]. To keep the required water pressure in the water network, engineers use EWTs, which increase the head of water in the network. Failure to these structures has a negative impact on the overall performance of the water network and degrade the resilience of water networks and consequently, the overall serving community (i.e. by increasing the potential of human losses and economic damages) after severe hazard such as seismic events. A review on the past earthquake demonstrates the vulnerability of EWTs having reinforced concrete shaft-type supports. For instance in 2001 Bhuj earthquake, three EWTs collapsed completely, and many more were damaged severely (Figure 1), and similar damages were observed in 1997 Jabalpur earthquake [5].

* Corresponding author: a.mellati@student.unsw.edu.au

http://dx.doi.org/10.28991/cej-03091177

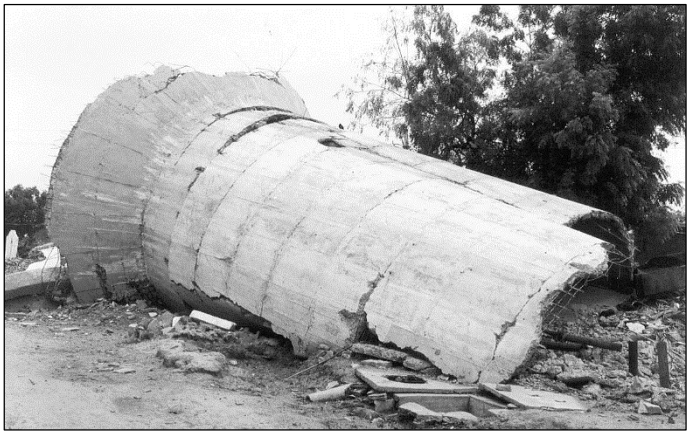

Figure 1. Collapsed 265 KL water tank in Chobari village about 20 km from the epicenter. The tank was approximately half full during the earthquake [6]

Nevertheless, few studies have been carried out on the dynamic behavior of EWTs. Evaluating the dynamic behavior of these structures contains complexities due to fluid-soil-structure interactions. Literature review indicates that paramount results are attainable. In the 1960s, Housner [7] proposed a method for simulating the hydrodynamic behavior of liquid in rectangular and cylindrical water tanks by introducing "impulsive" and "convective" masses. Moslemi et al. [5], by conducting a study on the seismic response of liquid-filled elevated tanks, indicated that the obtained masses using Housner equations yield a reasonable agreement in comparison to finite element method with at most 3% error. This method is recommended in some regulations such as Ref [8, 9] with some modifications.

It is the effect of soil-structure interaction (SSI) that is ignored in earlier studies [10], and [11]. Livaoğlu and Doğangün [12], by proposing simplified seismic analysis procedures for elevated tanks considering fluid-soil-structure interaction, indicate that the seismic design of reinforced concrete elevated tanks based on the simplified assumption that the subsoil is rigid or rock without any site investigation may lead to a wrong assessment of the seismic base shear and overturning moment. Dutta et al. [13] showed that the base shear of EWTs might be increased due to the impact of SSI. This study also clarified that ignoring the effect of SSI could result in potential large tensile forces in some of the staging columns due to seismic loads. Similar conclusions are emphasized by Ref [14].

Seismic assessment of structures can be performed accurately using rigorous finite element modeling and nonlinear response history analysis (NLRHA), which is time-consuming and computationally expensive [15]. Estimation of engineering demands parameters are the key to the performance-based engineering design [16], and the key to generating fragility curves, which is the main tool for high-level analysis such as community resilience planning and assessments [17-19]. An alternative to NLRHA is to use nonlinear static analysis (NSA) or pushover to estimate seismic demands parameters [20-22]. Pushover analyses are commonly used for seismic assessment of buildings and other structures [23]. Pushover curve relates the force and displacement demands in a structure such as base shears versus roof (i.e. top point) displacements. Another application of the pushover curve would be to identify design parameters such as overstrength factors for various structures [24].

This study proposes a new pushover procedure to estimate dynamic capacity curve (i.e. base shear versus top displacement) for EWTs considering both fluid and soil interactions with the main structure. NLRHA is used as a benchmark to obtain the mean dynamic capacity curve through incremental dynamic analysis (IDA) under an ensemble of ground motions. To generalize the proposed pushover procedure, the effect of different soil types according to Ref [15] on a EWT response with 150 m^3 capacity is evaluated. Then, the seismic behavior of this water tank is assessed under empty, third, two-thirds and full water level conditions. In addition, the influence of the tank capacity is investigated by considering four capacities: 150, 250, 350 and 450 m^3. Comparing the dynamic capacity curved obtained from the pushover with the benchmarks (i.e. dynamic capacity curved obtained from IDA) reveals the potential of the proposed pushover procedure for fast evaluation of EWTs. Moreover, this study could be a trigger for the performance-based seismic design of these structures.

2. Design and Modeling

2.1. Designing

For investigating the influences of soil type and water level parameters on seismic response of EWTs, a EWT with the capacity of 150 m^3 is designed due to Ref [8, 9] regulations. The seismic loads are applied through the design response spectrum in accordance with Ref [15] in San Diego, California. In the design process, it is assumed that the tank is located on soft soil type E according to Ref. [15], which is more critical than very dense soil [22, 25, 26]. Furthermore, the full and empty tank conditions are considered in order to control the occurrence of tensile stresses in the shaft [14]. As depicted in Figure 2, the tank is supported on a concrete shaft with an external diameter of 2.7 m, the

thickness of 0.35 m and the elevation of 20 m from top of the foundation ($H = 20$ m). External diameter of the cylindrical tank is 8 m with a thickness of 0.2 m and a tube-shaped duct with 1.5 m diameter ($d = 1.5$ m) is placed inside the tank for facilities purposes. The thicknesses of the bottom and roof tank slabs are 0.25 m and 0.2 m, respectively. The water height is supposed to be 3.1 m with 0.4 m free board. The structure is erected on a cylindrical foundation with a radius of 5 m and thickness of 1 m. The impact of tank capacity is assessed through similar tanks designed for capacities of 250, 350 and 450 m^3 in the same way. Table 1**Table** shows the geometric characteristic of the tanks.

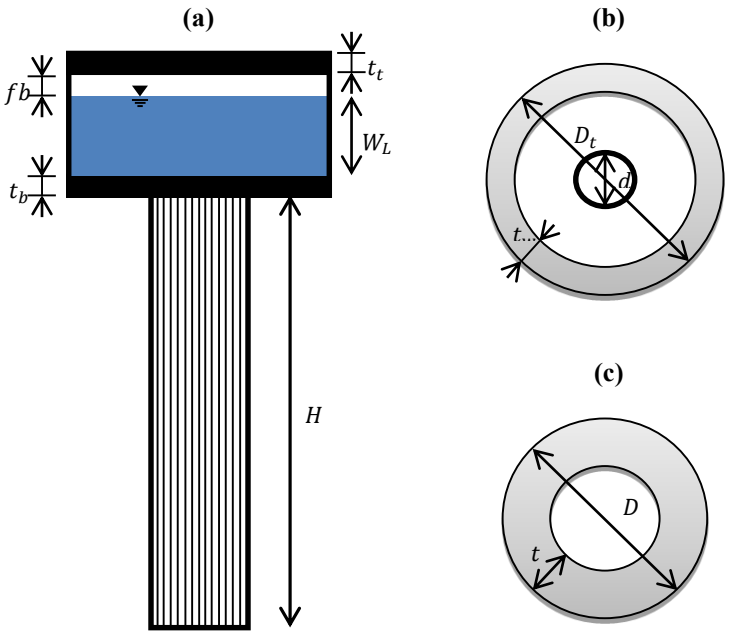

Figure 2. (a) Tank geometry shape; (b) Tank section; (c) Shaft section

Table 1. Tank geometry properties

Parameter (m)	Tank Capacity			
	150 m^3	**250 m^3**	**350 m^3**	**450 m^3**
D: Shaft external diameter	2.7	3	3.5	4
t: Shaft thickness	0.35	0.45	0.5	0.6
d: Internal tube-shaped duct	1.5	1.5	1.5	1.5
D_t: Tank diameter	8	9	10.5	11.5
t_w: Tank wall thickness	0.2	0.25	0.3	0.35
H: Shaft height	20	20	20	20
t_b: Bottom tank slab thickness	0.25	0.3	0.35	0.4
t_t: Top tank slab thickness	0.2	0.25	0.3	0.35
f_b: Free board	0.4	0.4	0.42	0.44
W_L: Water level	3.1	4.05	4.13	4.41
R: Foundation radius	5	6.5	7.5	8.5
h: Foundation thickness	1	1.3	1.5	1.7

Although the use of finite element method is commonplace in case studies, it is not applicable for parametric studies due to time-consuming and modelling complexities. Since, in this study, a lot of parameters are investigated through numerous nonlinear dynamic analyses, it is tried to model the structure simple enough to be useful in practical projects. The tank modelling is discussed in the following section.

2.2. Tank Modeling

The body of the tank including the top and bottom slabs and the side wall is assumed to be rigid and the mass of each part is centralized at a series of local points. This assumption offers identical rotational rigidity and total mass with the continuous model. A sequence of concentrated masses is utilized for equalizing the masses of top and bottom slabs as shown in Figure 3(a). The number of perimeter concentrated masses is equal to n_s. In this article, due to the symmetry of the structure, this parameter is taken to be 4. It is notable that augmenting the number of concentrated masses has

negligible effect on the responses in this case. For idealizing the masses, it is assumed that the summation of the concentrated masses is equal to the total mass of the slab, Equation 1, and total mass moment of inertia (around the radial axis passing through the volume center) is equal to the mass moment of inertia of concentrated masses (around the same axis), Equations 2-4. Using these assumptions, the amounts of concentrated masses can be obtain using Equations 5 and 6.

$$n_s m_{s,1} + m_{s,2} = M_s \tag{1}$$

$$I_1 = \int r^2 dm = \frac{M_s}{\pi R^2} \int_0^{2\pi} \int_0^R r^2 r dr d\theta = \frac{M_s R^2}{4} \tag{2}$$

$$I_2 = \frac{n_s m_{s,1} R^2}{2} \tag{3}$$

$$I_1 = I_2 \tag{4}$$

$$m_{s,1} = \frac{M_s}{2n_s} \tag{5}$$

$$m_{s,2} = \frac{M}{2} \tag{6}$$

Where M_s is the total slab mass $m_{s,2}$ is the equivalent concentrated mass at the center of the slab, and $m_{s,1}$ is the equivalent masses at the perimeter of the slab.

For idealizing the tank side wall, a series of concentrated masses is applied as depicted in Figure 3(b). The number of perimeter concentrated masses in each level is n_w, which is taken 4. Increasing the Parameter n_w has negligible effect on the result as noted earlier since the tank body is assumed to be rigid. Similar assumptions to the tank slab modelling lead to Equations 7 and 8.

$$m_{w,1} = \frac{M_w}{2n_w} \frac{6\left(\frac{R}{h}\right)^2 + 5}{6\left(\left(\frac{R}{h}\right)^2 + 1\right)} \tag{7}$$

$$m_{w,2} = \frac{M_w}{n_w} \frac{1}{6\left(\left(\frac{R}{h}\right)^2 + 1\right)} \tag{8}$$

Where M_w is the total mass of the side wall, $m_{w,2}$ is the equivalent perimeter mass at the middle level of the tank, $m_{w,1}$ is the equivalent perimeter mass at the top and bottom level of the tank, R is the tank radius, and h is the height of the tank.

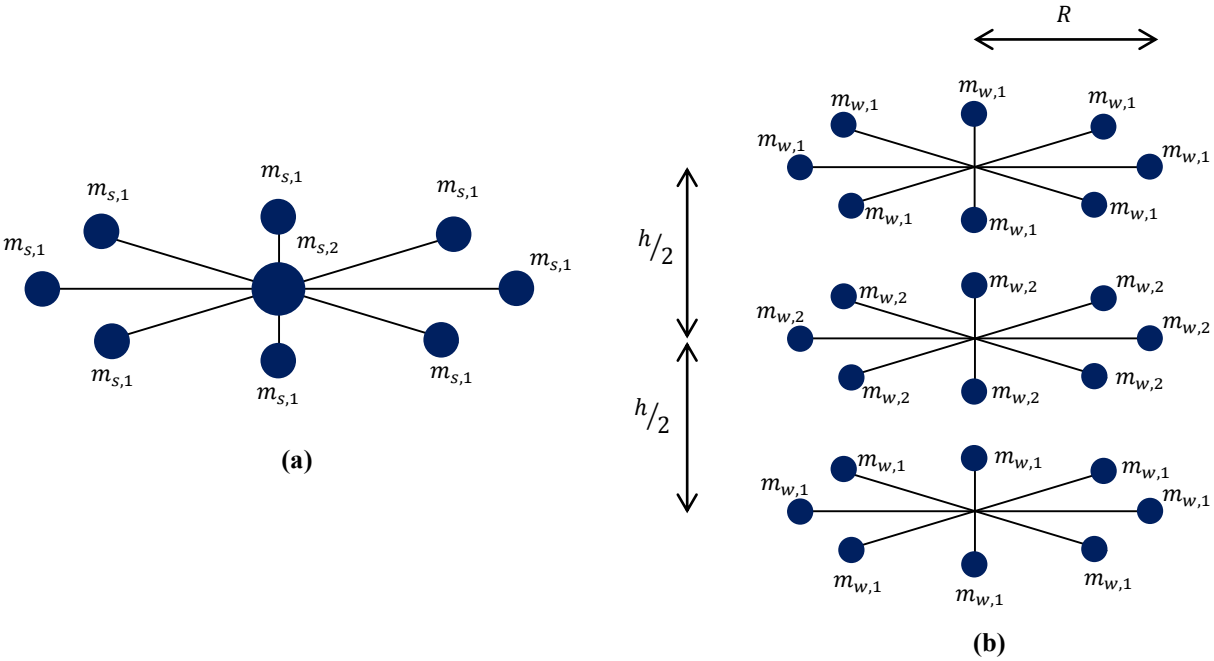

Figure 3. Equivalent concentrated masses. (a) Slabs; (b) Tank wall

The tank shaft is divided into 20 equal pieces and is modelled using frame elements. Plastic hinges are assigned at the beginning of each part according to Ref [27]. This assignment is utilized to provide nonlinear behavior along the shaft. The mass and the weight of each part is centralized in the middle of each part.

2.3. Fluid-Structure Interaction

Assuming the wall of the tank is rigid, modified Housner model [28] is used to consider fluid-structure interaction. In this model, according to Figure 4, the mass of the tank water is divided into two parts, impulsive and convective masses with the specific heights from the bottom of the tank. The impulsive mass (M_0) is considered to be rigid and connected to the tank wall by means of solid rods. The convective mass (M_1) is connected to the tank wall by two springs to reflect fluid-structure interaction with adequate accuracy in engineering problems. Masses, their height and springs stiffness of fluid-structure interaction model are calculated using Equations 9 to 13. In order to h_0 and h_1, shown in Figure 4, to consider the effect of water pressure on the bottom slab in addition to pressure on the side wall, it is recommended to take $\alpha = 1.33$ and $\beta = 2$; otherwise, it is recommended to take $\alpha = 0$ and $\beta = 1$ [28]. So, for elevated water tanks, $\alpha = 1.33$ and $\beta = 2$, were chosen. This fluid-structure interaction model is assessed and approved in Ref. [5]. This study assumes a rigid tank wall and slabs. More complicated version of the Housner model can be used to consider tank horizontal flexibility such as Ref [29] based on Haroun and Housner's model [30].

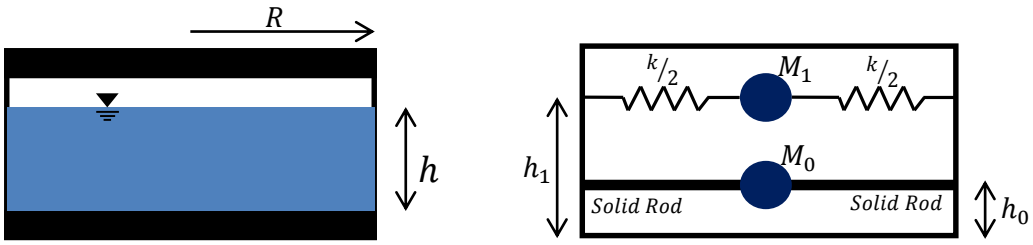

Figure 4. Fluid-structure interaction (Housner model)

$$M_0 = M\frac{\tanh 1.7\frac{R}{h}}{1.7\frac{R}{h}} \quad (9)$$

$$M_1 = \frac{0.71 \times \tanh 1.8\frac{h}{R}}{1.8\frac{h}{R}}M \quad (10)$$

$$k = \frac{4.75gM_1{}^2h}{MR^2} \quad (11)$$

$$h_0 = 0.38h\left(1 + \alpha\left(\frac{M}{M_0} - 1\right)\right) \quad (12)$$

$$h_1 = h\left(1 - 0.21\left(\frac{M}{M_1}\right)\left(\frac{R}{h}\right)^2 + 0.55\beta\frac{R}{h}\sqrt{0.15 \times \left(\frac{RM}{hM_1}\right)^2 - 1}\right) \quad (13)$$

Where M is the total mass of tank water, R is the radius of the tank, h is the height of the water, M_0 is the impulsive mass, M_1 is the convective mass, h_0 is the height of the impulsive mass from the bottom and h_1 is the height of convective mass from the bottom.

2.4. Soil-Structure Interaction

The well-known Cone model, shown in Figure 5, is used for modelling the effect of soil-structure interaction, which is described and assessed in several studies [22, 31-34]. This model assumes that foundation acts as a rigid body and the soil underneath is a homogeneous half-space. In this paper, the mass density of soil and concrete are assumed 1800 and 2500 kg/m^3, respectively. The Poisson coefficient of the soil is taken 0.3 and the tank geometric parameters are obtained from Table 1. Equations 14 to 18 show the soil parameters used in the Cone model.

$$A = \pi \times R^2 \quad (14)$$

$$M = Ah\rho_c \quad (15)$$

$$I_f = M\left(\frac{R^2}{4} + \frac{h^2}{3}\right) \quad (16)$$

$$V_p = V_s\sqrt{\frac{2(1-\nu)}{1-2\nu}} \quad (17)$$

$$k_h = \frac{8\rho {V_s}^2 R}{2-\nu} \quad (18)$$

$$k_\theta = \frac{8\rho {V_s}^2 R^3}{3(1-\nu)} \quad (19)$$

$$M_\theta = \frac{9\rho_c \pi R^5 (1-\nu)^2}{64(1-2\nu)} \quad (20)$$

$$c_h = \rho V_s A \quad (21)$$

$$c_\theta = \rho V_P I_f \quad (22)$$

Where R is the foundation radius, A is the foundation area, h is the foundation thickness, ρ_c is the concrete mass density, M is the foundation mass, I_f is the foundation mass moment of inertia, ν is the Poisson ratio, V_s is the soil shear wave velocity, V_P is the soil dilatational wave velocity, ρ is the soil mass density, k_h is the translational stiffness, k_θ is the rotational stiffness, M_θ is the mass of internal degree of freedom, c_h is the translational damping and c_θ is the rotational damping.

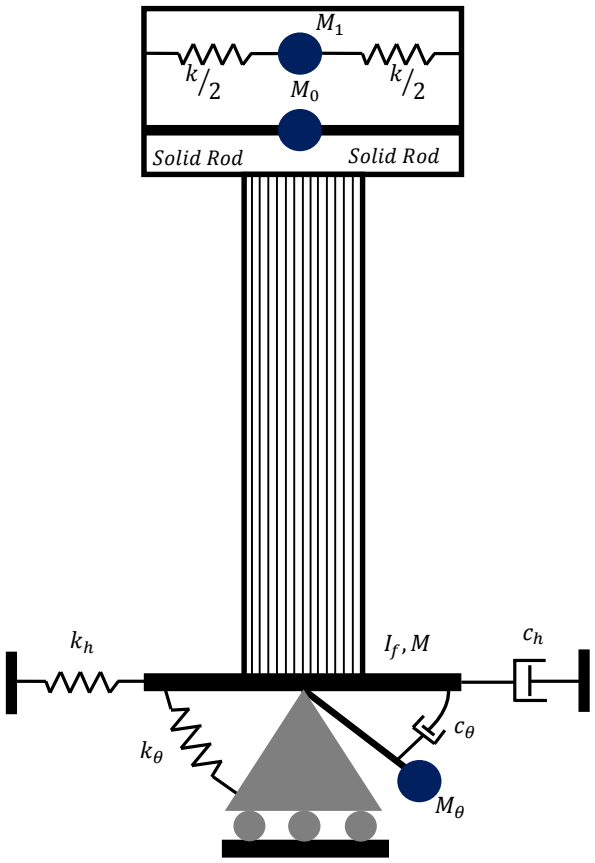

Figure 5. Soil-structure interaction (Cone model)

3. Ground motions and Analyses

The Far-Field record set [35] includes twenty-two records (44 individual components) selected from the PEER NGA database [36]. For each record, Table 2 summarizes the magnitude, year, and name of the event, as well as the name of

the station. These twenty-two records are taken from 14 events that occurred between 1971 and 1999. Of the 14 events, eight were California earthquakes and six were from five different other countries. Event magnitudes range from M6.5 to M7.6 with an average magnitude of M7.0 for the far-field records. This record set includes ground motions, recorded on the ground surface of either soft rock (site class C) or stiff soil (site class D) [35]. These records take no account of soft soils. To investigate the site effect with specific shear wave velocities, it is needed to modify the ground motion records. The procedure described in Ref [22] is used. A layer of granular soil with a thickness of 30m is assumed over a bedrock. According to the station of each earthquake record and its soil shear wave velocity, the characteristic of each component is achieved on the bedrock using equivalent linear method through ERRA program [37]. Then, having the soil shear velocity of the desired site, this procedure can be done reversely, and the ground motion records will be achieved on the ground surface in accordance with each specific soil. So, the far-field record set is modified based on the soil shear wave velocity of the site and scaled to different acceleration levels in order to use in IDAs. Figure 6 shows an example of a modified ground motion record for different soils.

Table 1. List of used ground motions [35]

Earthquake Name	Station Name	Site Class	V_s30 (m/s)	Com 1	Com 2	Year	PGA 1 (g)	PGA 2 (g)
Northridge	Beverly Hills - Mulhol	D	356	279	009	1994	0.516	0.416
Northridge	Canyon Country-WLC	D	309	270	000	1994	0.482	0.410
Duzce, Turkey	Bolu	D	326	090	000	1999	0.822	0.728
Hector Mine	Hector	C	685	090	000	1999	0.337	0.266
Imperial Valley	Delta	D	275	352	262	1979	0.351	0.238
Imperial Valley	El Centro Array #11	D	196	230	140	1979	0.380	0.364
Kobe, Japan	Nishi-Akashi	C	609	000	090	1995	0.509	0.503
Kobe, Japan	Shin-Osaka	D	256	000	090	1995	0.243	0.212
Kocaeli, Turkey	Duzce	D	276	270	180	1999	0.358	0.312
Kocaeli, Turkey	Arcelik	C	523	000	090	1999	0.216	0.150
Landers	Yermo Fire Station	D	354	270	360	1992	0.245	0.152
Landers	Coolwater	D	271	TR	LN	1992	0.417	0.283
Loma Prieta	Capitola	D	289	000	090	1989	0.529	0.443
Loma Prieta	Gilroy Array #3	D	350	000	090	1989	0.537	0.367
Manjil, Iran	Abhar	C	724	L	T	1990	0.515	0.496
Superstition Hills	El Centro Imp. Co.	D	192	000	090	1987	0.358	0.258
Superstition Hills	Poe Road (temp)	D	208	270	360	1987	0.446	0.300
Cape Mendocino	Rio Dell Overpass	D	312	360	270	1992	0.549	0.385
Chi-Chi, Taiwan	CHY101	D	259	N	E	1999	0.440	0.353
Chi-Chi, Taiwan	TCU045	C	705	N	E	1999	0.512	0.474
San Fernando	LA - Hollywood Store	D	316	090	180	1971	0.210	0.174
Friuli, Italy	Tolmezzo	C	425	000	270	1976	0.351	0.315

Using IDA for each component of the modified records, the IDA curves of the tanks are obtained by means of SAP2000 software. Firstly, the tank with 150 m^3 in full-filled status, which is located on different soil types with shear wave velocities of 175, 300, 550, and 1100 m/s, is investigated. Secondly, the tank with 150 m^3 located on the soft soil with shear wave velocity of 175 m/s is analyzed under different levels of water conditions, including empty, one-third, two-thirds and full-filled. Finally, the tanks with the capacities of 150, 250, 350 and 450 m^3, in full-filled water state placed on the soil with the shear wave velocity of 175 m/s, are studied.

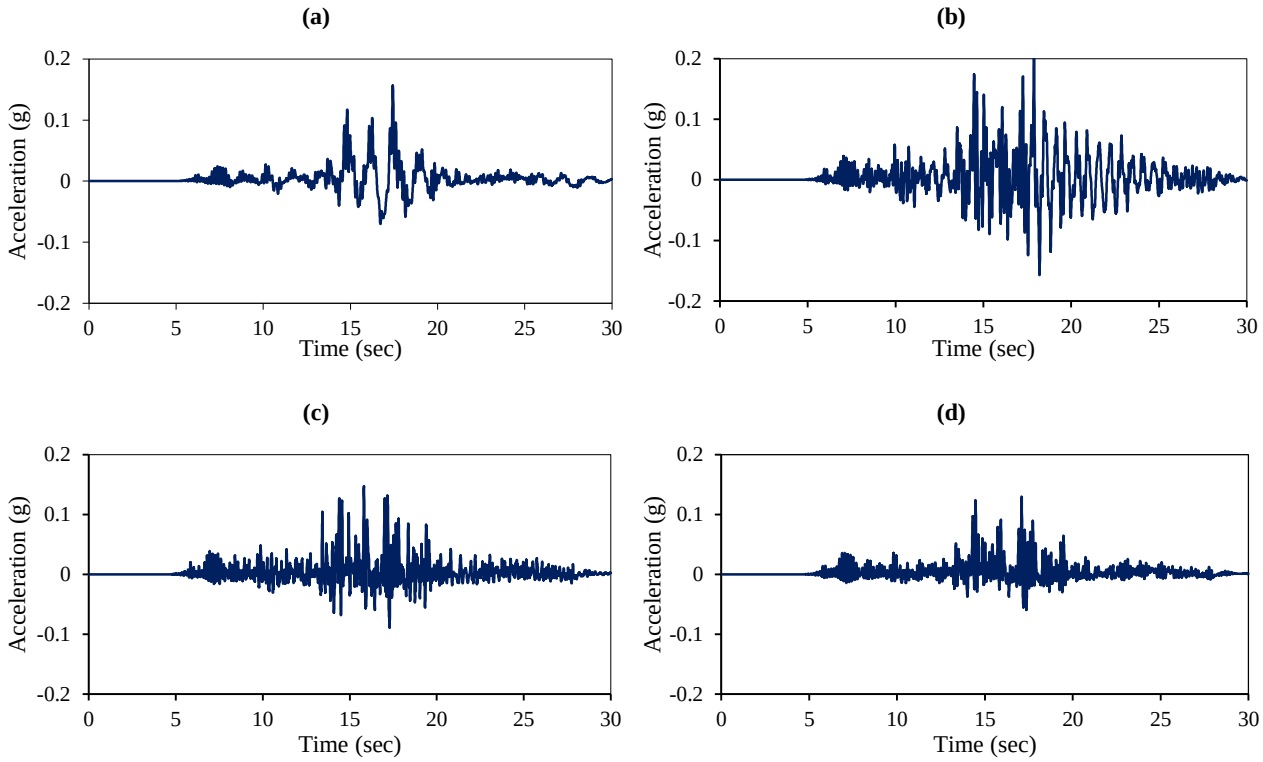

Figure 6. The time history of the modified acceleration for different soils; (a) 175 m/s; (b) 300 m/s; (c)550 m/s; (d) 1100 m/s.

4. Parametric Results

Figure 7(a) depicts the mean IDA curves of the elevated water tank with 150 m^3 capacity located on different soil types with shear velocities of 175 to 1100 m/s. As illustrated in this figure, with increasing the shear wave velocity of the soil, the tank shows less resistance. In other words, by changing the soil type from soft soil to rock, the ultimate base shear decreases, and it means ignoring the flexibility of soil in the design of these structures is conservative.

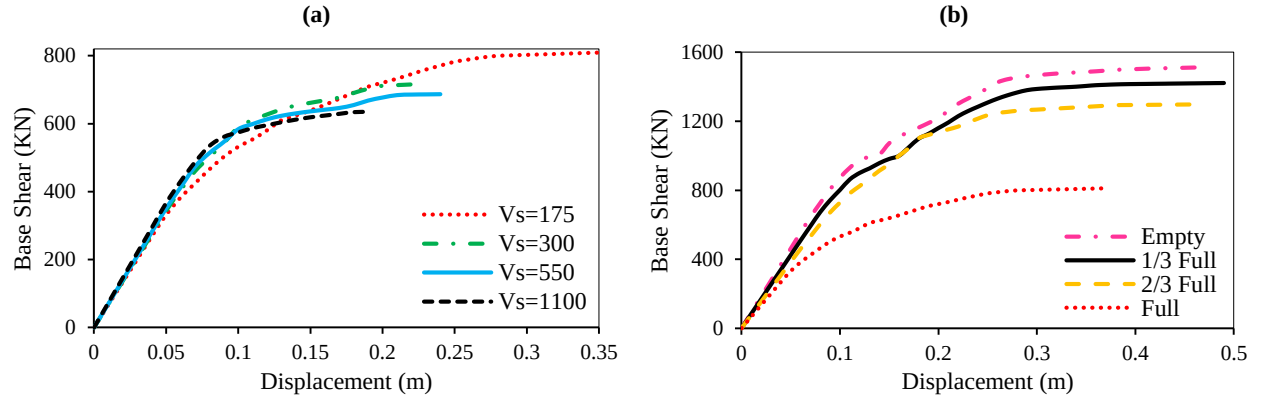

Figure 7. Dynamic capacity curves for the tank with 150 m^3 capacity; (a) different soil conditions in m/s; (b) different water level conditions

Figure 7(b) shows the tank mean IDA curves under different water levels for the tank with 150 m^3 capacity located on the soft soil with shear wave velocity of 175 m/s. As seen in this figure, by increasing the water level, the resistance of the tank reduces. In addition, as it is noticeable, there is a large gap between the full-filled state and the other states caused by hinge model behavior. In this model, the behavior of the hinges is determined by the ranges specified in Ref [27]. These ranges are distinguished based on the shear and axial forces in the hinge location. The water weight increases the axial force in the shaft. The additional weight of the full-filled water level compared to the two-thirds filled condition rises the axial force of the shaft. So, different hinge behavior is assigned to the hinges in the full-filled condition. Thus, these hinges have lower ductility behavior, which they lead to the gap between the full-filled condition and other states. Figure 8 displays the mean IDA curve for various tank capacities. As it is clarified, by increasing the tank capacity, the tank resistance is amplified. Since, by increasing the designed applied forces, the stiffness and the capacity of the shaft increase.

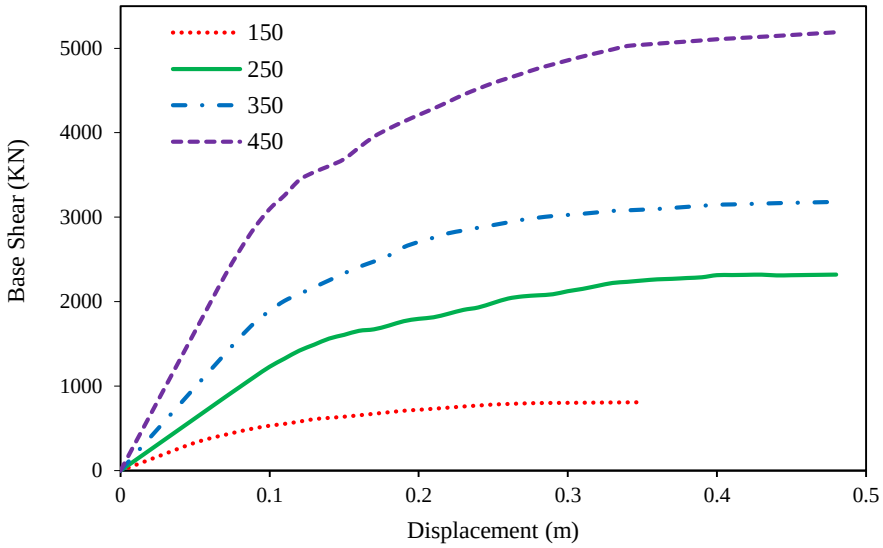

Figure 8. Dynamic capacity curves for the tank with different capacities in m^3

5. Proposed Pushover Procedure

Conducting a series of pushover analyses with common lateral load patterns and using NLRHA, as an exact solution, a pushover procedure is suggested, which is compatible with mean IDA curves of structures obtained from IDAs. This procedure contains two individual linear and nonlinear parts; (1) Linear part is appropriate for the initial part of the mean IDA curve (i.e. when the structural behavior is linear) and (2) the nonlinear part, containing (a) Initial and (b) Secondary load patterns, is suitable for the nonlinear part of mean IDA curve (i.e. when the structural behavior is inelastic). By adjoining the diagram obtained from linear part (i.e. part (1)) and the diagram obtained from secondary load pattern (i.e. part (b)), the structural mean IDA curve could be estimated as illustrated in Figure 9(a). In all cases, gravity loads are applied first and pushover analyses are carried out afterward.

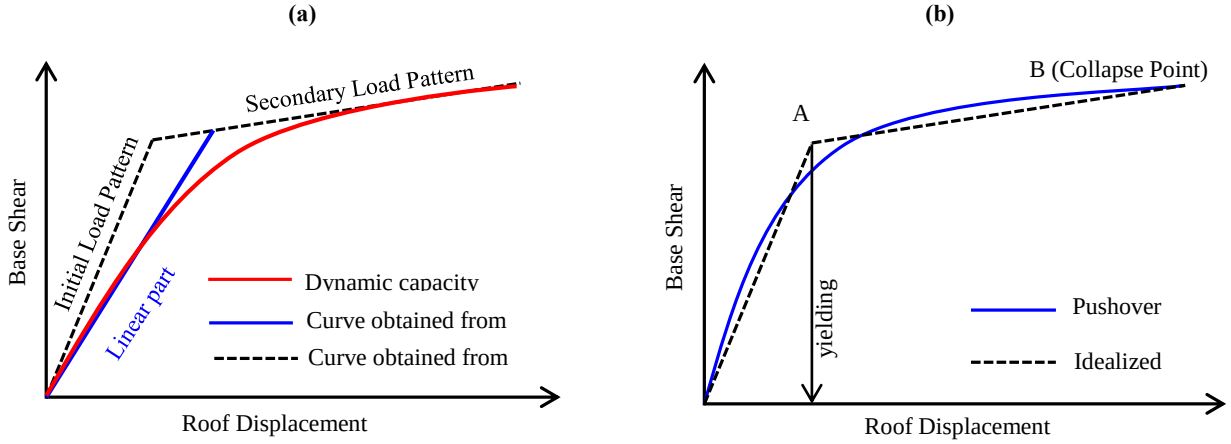

Figure 9. (a) Linear and Nonlinear parts; (b) Idealizing pushover curve and the yielding displacement

5.1. Linear part

For the linear part, appropriate load patterns by knowing the soil type and ratio of tank seismic mass to shaft mass (MR), are as follow. It is remarkable that tank seismic mass includes the tank mass, the convective mass, and the impulsive mass.

If the tank is located on soil type D or harder (i.e. larger shear wave velocity), the appropriate lateral load pattern is a concentrated force at the tank center of mass, Figure 10(a). This is regardless of MR and water level conditions. If the tank is located on soil type E or softer (i.e. smaller shear wave velocity), (1) for the case when the MR is equal or less than 2 (i.e. MR≤2) the pertinent lateral load pattern is the uniform load Figure 10(b) and (2) for the case when the MR is greater than 2 (i.e. MR>2) the suitable lateral load pattern is a combined load Figure 10(c). Combined load pattern is obtained from a combination of uniform and triangular loads. These load patterns are regardless to water level conditions.

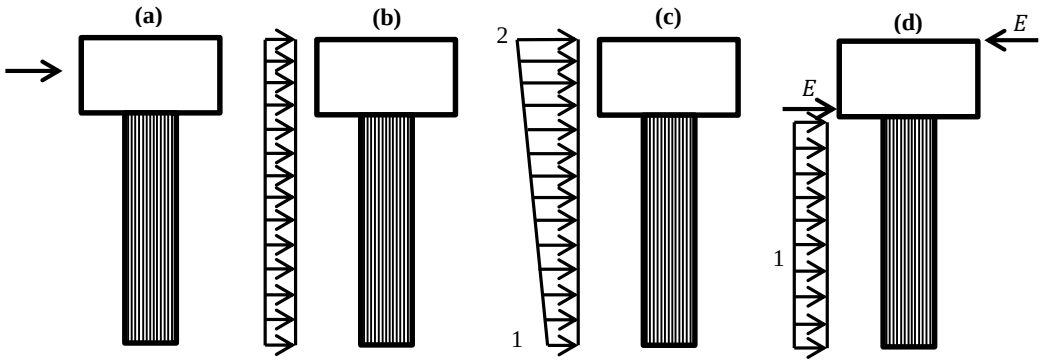

Figure 10. (a) Concentrated; (b) Uniform; (c) Combined load pattern; (d) proposed load pattern.

5.2. Nonlinear part

In order to determine the nonlinear part of the load pattern (i.e. part 2), a two-phase pushover analysis is required. First, the structure is pushed using the Initial load pattern as described in section 5.2.1. Then, the resulting curve is idealized to the bilinear diagram as described in Ref [38]. This results in the corresponding yielding displacement, point A in Figure 9(b). Preserving the first part of the pushover results (i.e. up to point A), the structure should be pushed from point A using the secondary load patterns as described in section 5.2.2. A reader is referred to Ref [22] for more details on performing consecutive pushover analyses. The curve obtained by secondary load pattern is suitable for the nonlinear part of the mean IDA curve.

5.2.1. Initial Load Pattern

The appropriate *Initial* load pattern, used for the nonlinear part, can be obtained by the knowledge of the soil type and MR as follow:

(1) If the tank is located on soil type D or harder, the proper lateral load pattern will be the combined load pattern as illustrated in Figure 10(c). This is regardless of MR and water level conditions. As noted before, the combined load pattern is obtained from a combination of uniform and triangular loads.

(2) If the tank is located on soil type E or softer, (a) when the MR is equal or less than 2 (i.e. MR≤2) the pertinent lateral load pattern is the uniform load as illustrated in Figure 10(b), and (b) when the MR is greater than 2 (i.e. MR>2) the suitable lateral load pattern is the combined load as illustrated in Figure 10(c). This is regardless of water level conditions.

5.2.2. Secondary Load Pattern

The appropriate secondary load pattern, used for the nonlinear part, can be obtained by the knowledge of the water level condition and MR as follow:

(1) If the MR is equal or less than 2 (i.e. MR≤2); (a) when the tank is full, the proposed load pattern as illustrated in Figure 10(d) should be used, and, (b) when the tank is not full (i.e. empty, one third, and two-thirds full), the uniform load pattern as illustrated in Figure 10(b) should be used.

(2) If the MR is greater than 2 (i.e. MR>2) ; (a) when the tank is full, the proposed load pattern as illustrated in Figure 10(d) should be used, and, (b) when the tank is not full (i.e. empty, one third, and two-thirds full), the combined load pattern as illustrated in Figure 10(c) should be used.

In the proposed load pattern, Figure 10(d), parameter E is given by:

$$E = L \times \frac{M_T + M_0 + M_1}{M_S} \quad (23)$$

Where L is shaft length, M_T is tank mass, M_0 is impulsive mass, M_1 is convective mass, and M_S is shaft mass.

5.3. Step-by-Step Summary (Figure 12)

(1) Apply gravity loads.

(2) Preserving the gravity condition, develop the base shear - reference displacement pushover curve by applying the appropriate load pattern from Section 05.1.

(3) Idealize the obtained pushover curve from Step (2)2, as bilinear and keep the results of the first branch as the linear part results.

(4) Apply gravity loads to a new unloaded model.

(5) Preserving the gravity condition, develop the base shear - reference displacement pushover curve by applying the appropriate load pattern from Section 5.2.1.

(6) Idealize the obtained pushover curve from Step 5, as bilinear to obtain the yielding displacement (i.e. point A in Figure 9(b)).

(7) Apply gravity loads to a new unloaded model.

(8) Preserving the gravity condition, develop the base shear - reference displacement pushover curve by applying the same load pattern from Step 5 till the displacement reach to point A obtained in Step 6.

(9) Preserving the results of the Step 8, push the structure by applying the appropriate load pattern from Section 5.2.2 and keep the second part of this step.

(10) Adjoin the resulted pushover curves from Steps 3 and 9 leads to the estimated mean IDA curve as illustrated in Figure 11.

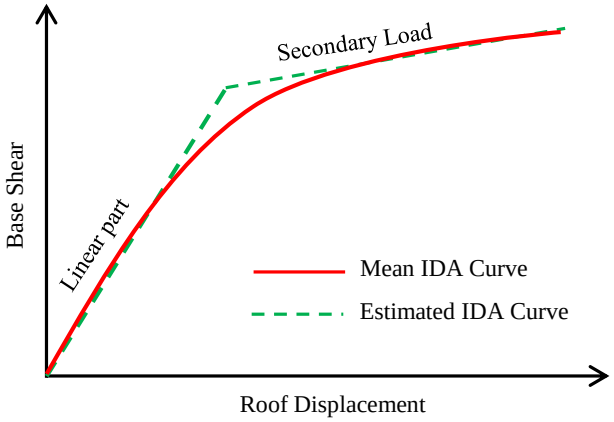

Figure 11. Estimated capacity curve

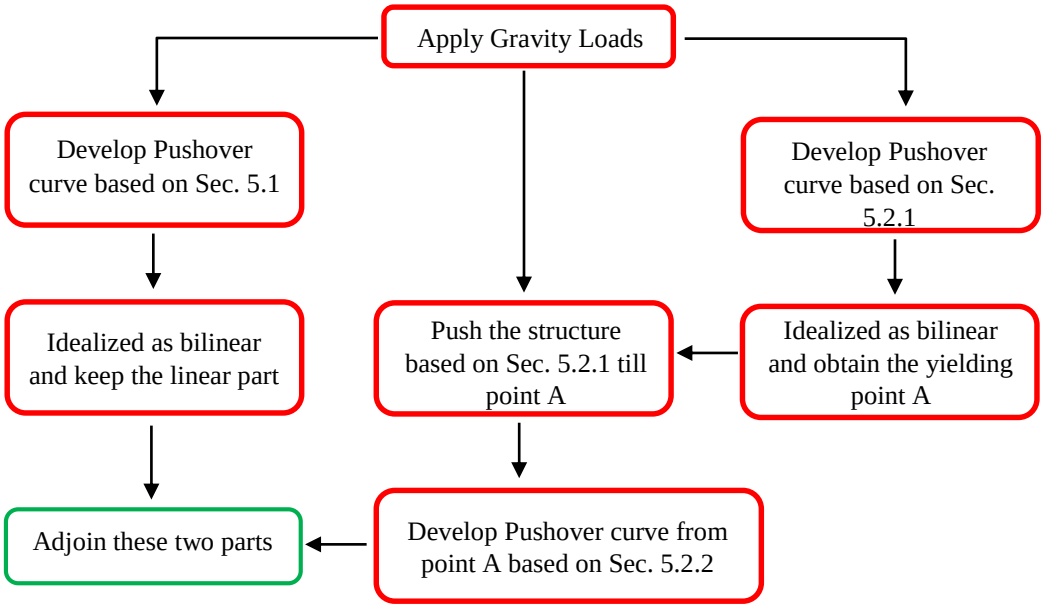

Figure 12. The flowchart of the proposed pushover procedure

6. Evaluation of the Proposed Pushover Procedure

In this section, the proposed pushover procedure is evaluated on the studied EWTs. The estimated IDA curves (dynamic capacity curves) for the tanks with 150 m^3, full water level condition, located on different soil types are presented in Figure 13, and the errors of these estimations are presented in Figure 14(a).

As can be seen in Figure 14(a), the proposed pushover procedure has a good estimation of the IDA curves with maximum errors less than 30%. It should be noted that the largest errors are related to the transition parts between the linear (i.e. the first) part of the IDA curves and the nonlinear (i.e. the last) part of the IDA curves. Away from the transition parts, the errors are less than 7%. Moreover, the IDA curves ± one standard error are also plotted to better show the reasonability of the estimated IDA curves.

The estimated IDA curves (dynamic capacity curves) for the tanks with 150 m^3, located on soil with the shear wave velocity of 175 m/s, with different water level conditions are presented in Figure 15 and the errors of these estimations are presented in Figure 14(b). Similar trends to Figure 13, for various soil types, can be observed for various water level. However, as can be seen in Figure 14(b), the errors outside of the transition parts are increasing as the water level decreases. These errors (outside of the transition parts) are 6.30, 7.30, 15.91, and 22.88% for the full, two-thirds, one-third, and empty tanks, respectively. Overall, the estimations are satisfactory.

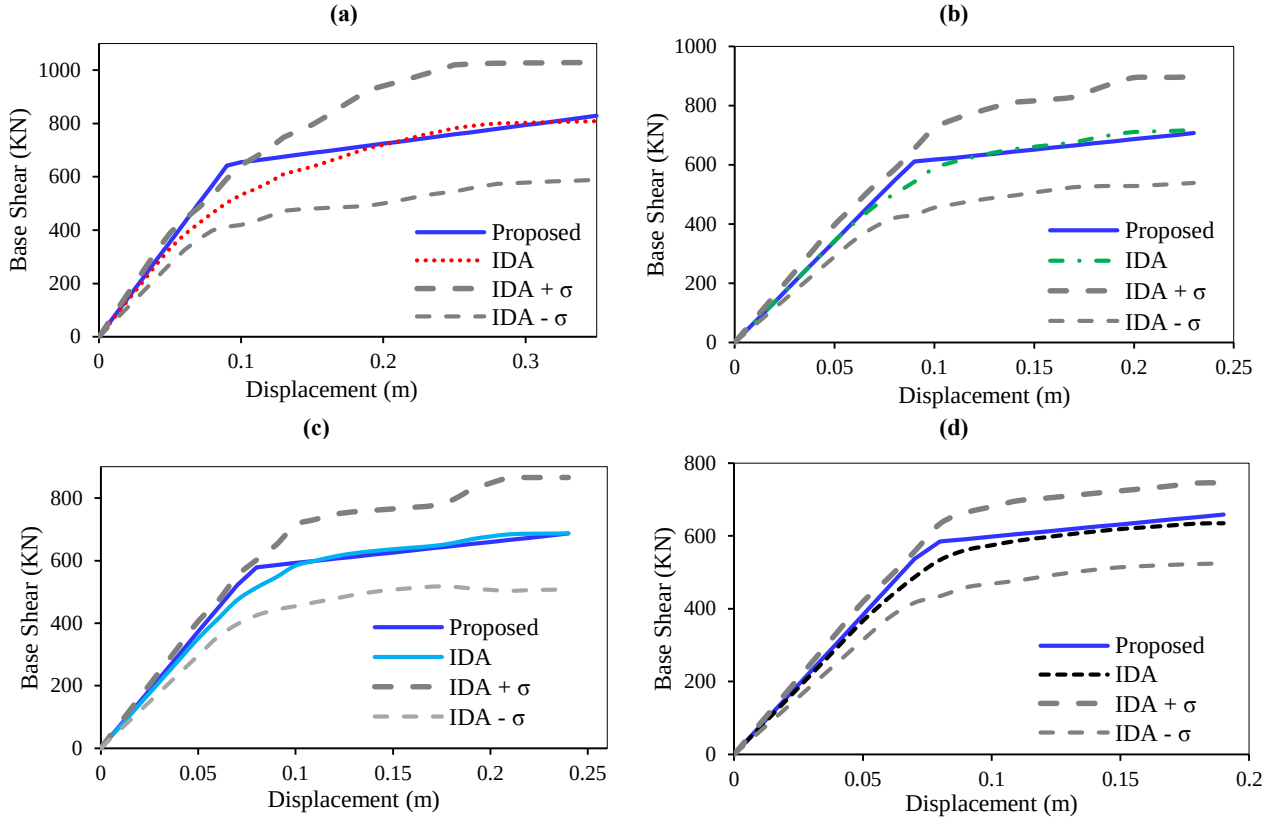

Figure 13. Estimated dynamic capacity curves for the tanks with 150 m^3 capacity and full water level on the soil with the shear wave velocities of; (a) 175 m/s; (b) 300 m/s; (c) 550 m/s; and (d) 1100 m/s

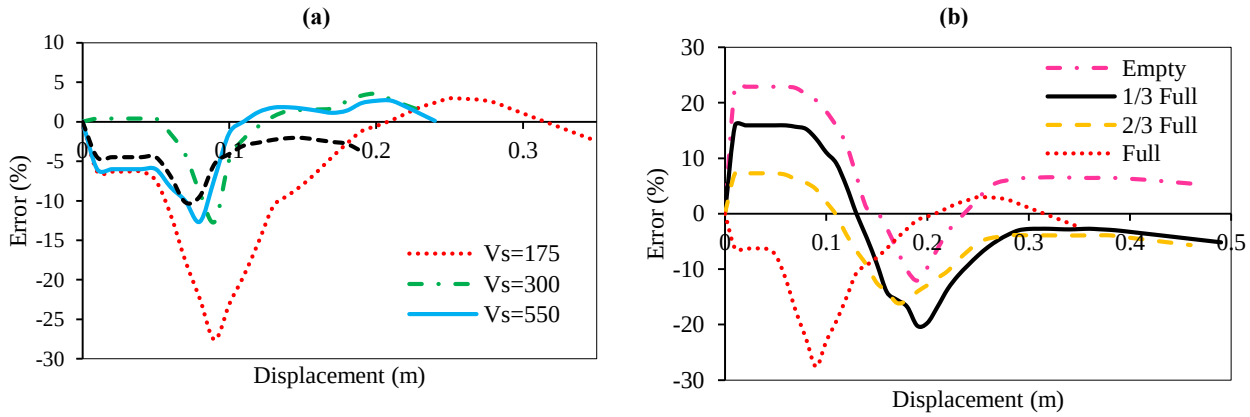

Figure 14. Errors in the estimation of the dynamic capacity curves for the tank with 150 m^3 capacity; (a) different soil conditions in m/s; (b) different water level conditions

The estimated IDA curves (dynamic capacity curves) for various tank capacities, located on the soil with the shear wave velocity of 175 m/s, with full water level conditions are presented in Figure 16 and the errors of these estimations are presented in Figure 17. As can be seen in Figure 10, the maximum errors of these estimations are limited to below 30%, which are related to the transition part. The estimation errors for the linear (i.e. first) part increases by the increase

in the tank capacity (i.e. stiffer and stronger shaft). These errors for the first part are 6.30, 12.27, 12.23, and 21.87% for tanks with capacities of 150, 250, 350, and 450 m^3, respectively. The estimation errors of the nonlinear part are less than 10%.

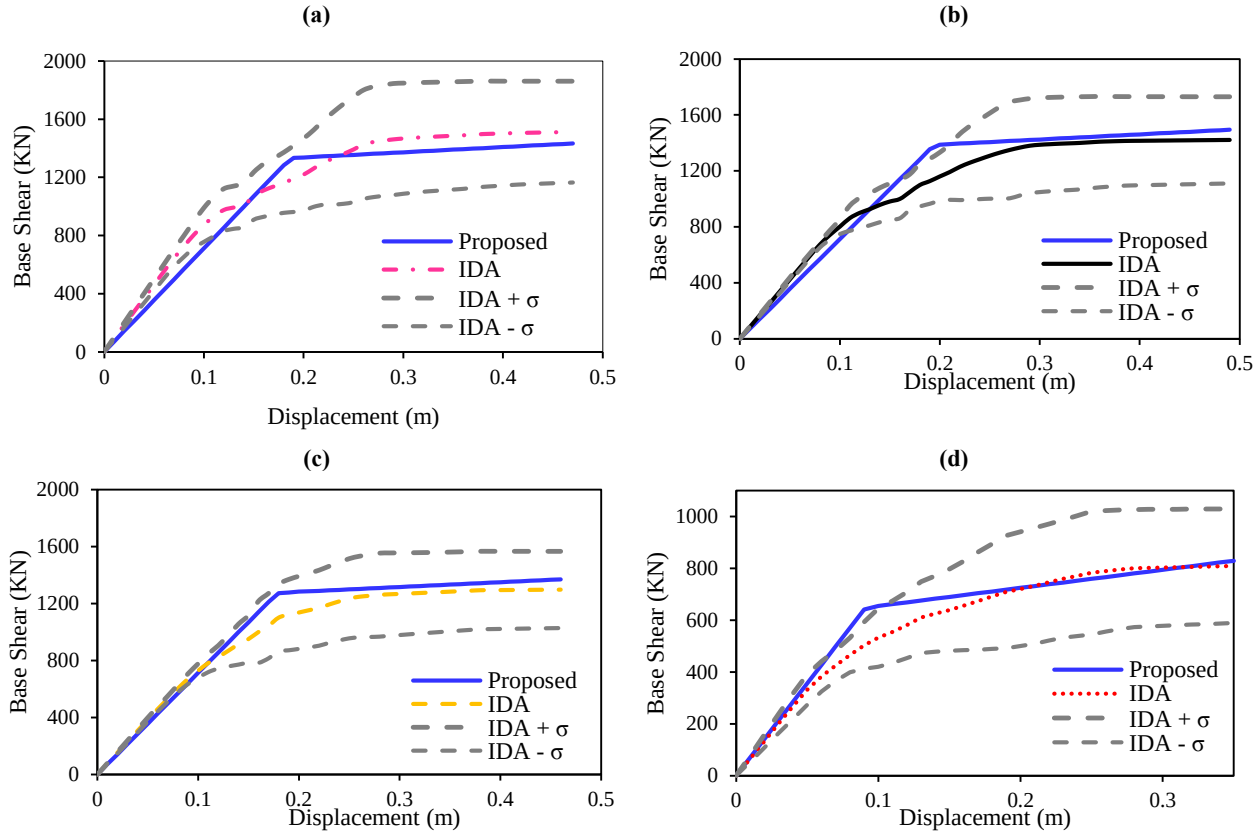

Figure 15. Estimated dynamic capacity curves for the tanks with 150 m^3 capacity on the soil with the shear wave velocity of 175 m/s with the water level of; (a) empty; (b) one-third full; (c) two-thirds full; and (d) full

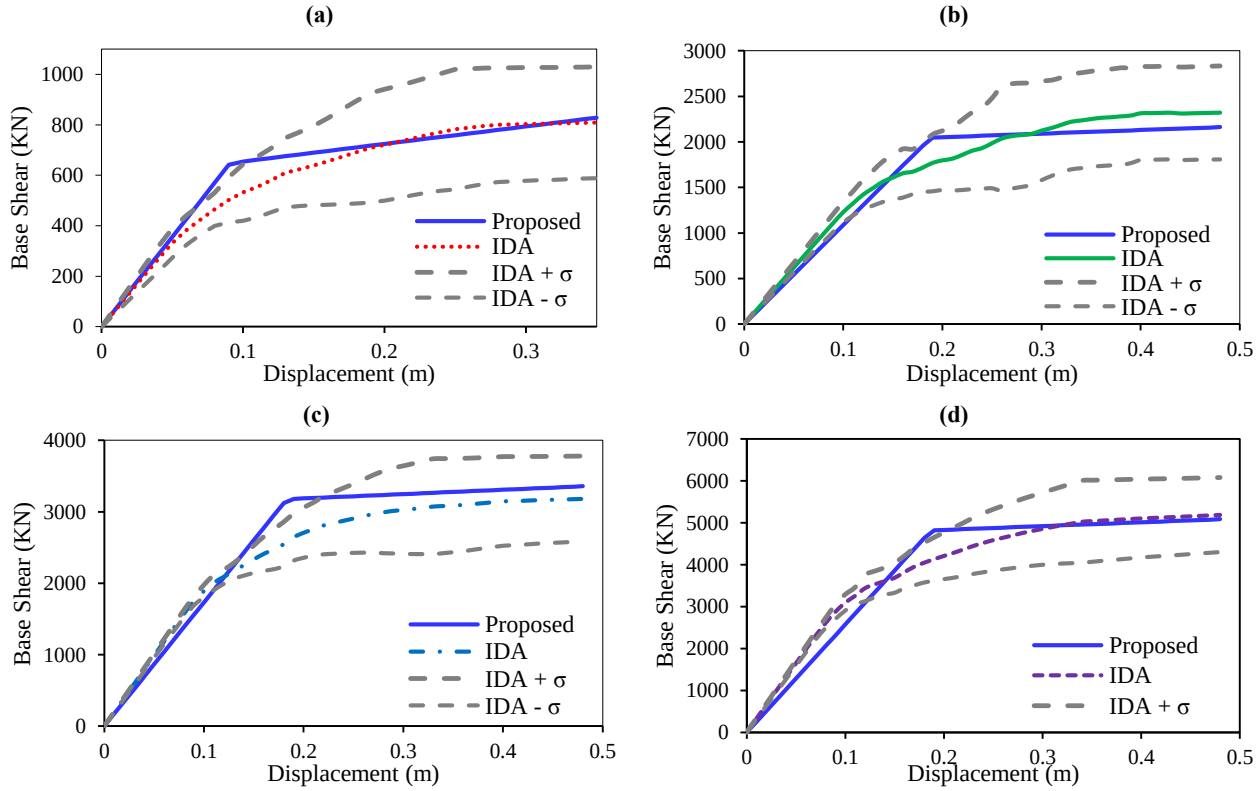

Figure 16. Estimated dynamic capacity curves for the tanks with full water level and on the soil with the shear wave velocity of 175 m/s with capacities of; (a) 150 m^3; (b) 250 m^3; (c) 350 m^3; and (d) 450 m^3

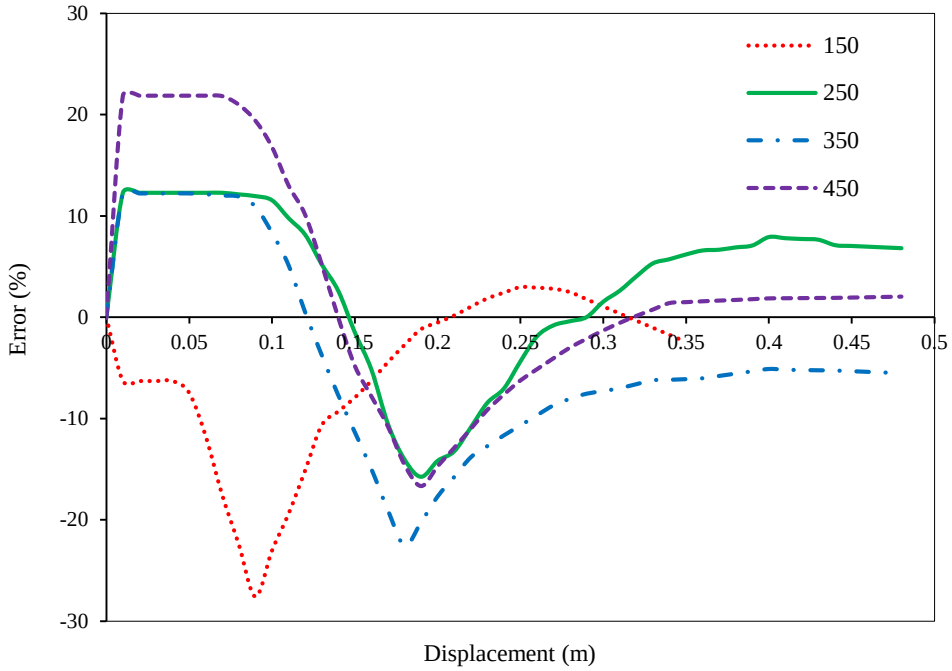

Figure 17. Errors in the estimation of the dynamic capacity curves for the tank with different capacities in m^3

7. Conclusion

In this paper, a new pushover procedure is presented to estimate the mean incremental dynamic analysis curve (i.e., base shear versus reference displacement) for an elevated water tank supported on concrete shaft. This procedure is based on two separate pushover analyses. The first pushover analysis is intended to estimate the linear part of the IDA curve, section 05.1. The second pushover analysis, which is a two-phase consecutive pushover analysis, is intended to estimate the nonlinear part of the IDA curve, where the second phase is the estimation of the nonlinear part of the IDA curve. Finally, the estimated IDA curve is obtained by adjoining the linear part and the second phase of the nonlinear part of the proposed pushover procedure. In the modelling of the tank, the effect of soil-structure interaction is considered through the Cone model, and the effect of fluid-structure interaction is considered through the Housner model. For simplicity, the shaft is modelled using frame elements with plastic hinges distributed along the shaft for considering the nonlinearity.

A comprehensive parametric study is performed by varying soil types, water level conditions and tank capacities to better understand the behavior of elevated water tanks. It has been observed that an increase in the shear wave velocity of the soil, which is equivalent to soil hardening, decreases the structural resistance due to soil-structure interaction. The structure behavior is sensitive to the soil type; hence, it is recommended to perform an assessment to determine the soil type in practical projects. Moreover, the results show that by increasing the tank capacity and shaft stiffness, structure dynamic capacity (IDA curve) increases; however, in the shaft with large dimension, the potential of brittle collapse increases, and more precautions should be considered. In addition, by a reduction in the water level, the potential of collapse reduces, and the structural resistance increases, subsequently, due to a decrease of seismic mass and reduction of shaft axial force. Comparing the IDA curves for different water level conditions, it is concluded that, the full-filled water level is the critical one. However, in practice, it is suggested to control the empty tank because of the higher potential of occurring tensile stresses. The result of this parametric study can be used to generate fragility curves for the assessed conditions.

The proposed pushover procedure based on suggested lateral load patterns predicts the mean IDA curve of EWTs with ample accuracy. The estimation errors are below 30%, which are related to the transition area between the linear and nonlinear parts. Away from the transition area, the errors of the proposed pushover procedure reduce. In the future, the more complex modelling, which would be a more realistic representation of the model should be considered. This can be accomplished by using finite element modelling of the shaft and the tank instead of frame elements, more rigorous nonlinear soil-structure interaction, and fluid-structure interaction.

8. Conflicts of Interest

The authors declare no conflict of interest.

9. References

[1] Nourbakhsh-Rey, Mehrnoush, and Marc Libault. "Decipher the Molecular Response of Plant Single Cell Types to Environmental Stresses." BioMed Research International 2016 (2016): 1-8. doi: 10.1155/2016/4182071.

[2] Salahshoor, Shadi, and Mashhad Fahes. "Experimental Determination of the Phase Transition Point in Gas Condensates Using a Cost-Effective Semiautomated Isochoric Apparatus." SPE Western Regional Meeting (2018). doi:10.2118/190102-ms.

[3] Salahshoor, S., Mashhad F., and Catalin T. "A review on the effect of confinement on phase behavior in tight formations." Journal of Natural Gas Science and Engineering (2017) doi: 10.1016/j.jngse.2017.12.011.

[4] Salahshoor, Shadi, and Mashhad Fahes. "A Study on the Factors Affecting the Reliability of Laboratory-Measured Gas Permeability." Abu Dhabi International Petroleum Exhibition & Conference (2017). doi:10.2118/188584-ms.

[5] Moslemi, M., M.R. Kianoush, and W. Pogorzelski. "Seismic Response of Liquid-Filled Elevated Tanks." Engineering Structures 33.6 (2011): 2074-2084. doi: 10.1016/j.engstruct.2011.02.048.

[6] Rai, D.C. "Performance of Elevated Tanks in Mw 7.7 Bhuj Earthquake of January 26th, 2001." Journal of Earth System Science 112.3 (2003): 421-429. doi: 10.1007/BF02709269.

[7] Housner, G.W. "The Dynamic Behavior of Water Tanks." Bulletin of the seismological society of America 53.2 (1963): 381-387.

[8] ACI 350.3-06. "Seismic Design of Liquid-Containing Concrete Structures and Commentary" (2006) American Concrete Institute.

[9] ACI 371R-16. "Guide for Analysis, Design, & Construction of Elevated Concrete & Composite Steel-Concrete Water Storage Tanks" (2016) American Concrete Institute.

[10] GOTO, Yozo, and Takeshi Shirasuna. "Studies On Sh Wave Input Earthquake Responses of Grouped Underground Tanks In Soft Ground." Proceedings of the Japan Society of Civil Engineers 1983, no. 340 (1983): 1–10. doi:10.2208/jscej1969.1983.340_1.

[11] Doğangün, A., and R. Livaoğlu. "Hydrodynamic Pressures Acting on the Walls of Rectangular Fluid Containers." Structural Engineering and Mechanics 17.2 (2004): 203-214. doi: 10.12989/sem.2004.17.2.203.

[12] Livaoğlu, R., and A. Doğangün. "Simplified Seismic Analysis Procedures for Elevated Tanks Considering Fluid-Structure-Soil Interaction." Journal of fluids and structures 22.3 (2006): 421-439. doi: 10.1016/j.jfluidstructs.2005.12.004.

[13] Dutta, S., A. Mandal, and S.C. Dutta. "Soil-Structure Interaction in Dynamic Behaviour of Elevated Tanks with Alternate Frame Staging Configurations." Journal of Sound and Vibration 277.4-5 (2004): 825-853. doi: 10.1016/j.jsv.2003.09.007.

[14] Dutta, S.C., S. Dutta, and R. Roy. "Dynamic Behavior of R/C Elevated Tanks with Soil-Structure Interaction." Engineering Structures 31.11 (2009): 2617-2629. doi: 10.1016/j.engstruct.2009.06.010.

[15] ASCE/SEI 7-10. "Minimum Design Loads for Buildings and Other Structures" (2010), American Society of Civil Engineers.

[16] Tehrani, M.H., P.S. Harvey Jr., H.P. Gavin, and A.M. Mirza. "Inelastic Condensed Dynamic Models for Estimating Seismic Demands for Buildings." Engineering structures 177(2018) 616-629. doi: 10.1016/j.engstruct.2018.07.083.

[17] Zhang, W., N. Wang, C.D. Nicholson, and M. Hadikhan Tehrani. "A Stage-wise Decision Framework for Transportation Network Resilience Planning." arXiv (2018). arXiv:1808.03850.

[18] Zhang, W., N. Wang, C.D. Nicholson, and M. Hadikhan Tehrani "Stage-wised Resilience Planning for Transportation Networks." 12th International Conference on Structural Safety & Reliability - ICOSSAR (2017).

[19] Tehrani, M.H., A.D. Rodriguez Castillo, N. Wang, and C.D. Nicholson. "A Data-driven Framework for Hazard-sensitive Infrastructure Component Importance Ranking." Reliability Engineering and System Safety (2019).

[20] Hadikhan Tehrani, M., A. Mellati, and F. Khoshnoudian. "New Lateral Load Pattern for Estimating Seismic Demands of Elevated Water Tanks Supported on Concrete Shaft." International Conference on Advances in Structural, Civil, and Environmental Engineering - SCEE (2013).

[21] Hadikhan Tehrani, M., A. Mellati, M. Fallahian, and F. Khoshnoudian. "Evaluation of Different Lateral Load Patterns in Estimating Seismic Demands of 3D Mass Eccentric Mid-rise Building." International Conference on Advances in Structural, Civil, and Environmental Engineering - SCEE (2013).

[22] Hadikhan Tehrani, M., and F. Khoshnoudian. "Extended Consecutive Modal Pushover Procedure for Estimating Seismic Responses of One-way Asymmetric Plan Tall Buildings Considering Soil-Structure Interaction." Earthquake Engineering and Engineering Vibration, 13.3. (2014): 487-507. doi: 10.1007/s11803-014-0257-6.

[23] Ait L'Hadj, L., Hammoum, H., Bouzelha, K. "Nonlinear analysis of a building surmounted by a reinforced concrete water tank under hydrostatic load." Advances in Engineering Software, 117. (2018): 80-88. doi: 10.1016/j.advengsoft.2017.04.005.

[24] Mellati. A., M. Hadikhan Tehrani, Y. H. Zeinali, M. Banazadeh and F. Paytam. "Evaluation of Overstrength Factor of Steel Moment Resisting Frames." International Conference on Advances in Structural, Civil, and Environmental Engineering - SCEE (2013).

[25] Livaoğlu, R., and A. Doğangün. "Effect of Foundation Embedment on Seismic Behavior of Elevated Tanks Considering Fluid–Structure-Soil Interaction." Soil Dynamics and Earthquake Engineering 27.9 (2007) 855-863. doi: 10.1016/j.soildyn.2007.01.008.

[26] Masaeli, H., F. Khoshnoudian, and M. Hadikhan Tehrani. "Rocking Isolation of Nonductile Moderately Tall Buildings Subjected to Bidirectional Near-fault Ground Motions." Engineering Structures 80 (2014): 298-315. doi: 10.1016/j.engstruct.2014.08.053.

[27] ASCE/SEI 41-13. "Seismic Evaluation and Retrofit of Existing Buildings" (2013) American Society of Civil Engineers.

[28] Newmark N.M., and E. Rosenblueth. "Fundamental of Earthquake Engineering." (1971).

[29] Fallahian, M., A. Mellati, M. Hadikhan Tehrani, F. Khoshnoudian and M. Tarverdi "Parametric Analysis of Liquid Storage Tanks Base Isolated by Double Concave Friction Pendulum System", International Conference on Advances in Structural, Civil, and Environmental Engineering - SCEE (2013).

[30] Haroun, M.A., and G.W. Housner. "Seismic design of liquid storage tanks." Journal of the Technical Councils of ASCE 107.1 (1981): 191-207.

[31] Wolf, John P., and Andrew J. Deeks. "Introduction." Foundation Vibration Analysis (2004): 1–9. doi:10.1016/b978-075066164-5/50003-4.

[32] Khoshnoudian, F., E. Ahmadi, M. Kiani, and M. Hadikhan Tehrani. "Dynamic Instability of Soil-SDOF Structure Systems under Far-fault Earthquakes." Earthquake Spectra 31.4 (2015): 2419-2441. doi: 10.1193/062613EQS170M.

[33] Khoshnoudian, F., E. Ahmadi, M. Kiani, and M. Hadikhan Tehrani. "Collapse Capacity of Soil-Structure Systems under Pulse-like Earthquakes." Earthquake Engineering & Structural Dynamics 44.3 (2015): 481-490. doi: 10.1002/eqe.2501.

[34] Ghannad, M.A., and H. Jahankhah. "Site-dependent Strength Reduction Factors for Soil-Structure Systems." Soil Dynamics and Earthquake Engineering 27.2 (2007): 99-110. doi: 10.1016/j.soildyn.2006.06.002.

[35] FEMA P695. "Quantification of Building Seismic Performance Factors" (2009) Federal Emergency Management Agency.

[36] PEER. "Pacific Earthquake Engineering Research Center" http://peer.berkeley.edu/

[37] EERA. "A Computer Program for Equivalent-linear Earthquake site Response Analyses of Layered Soil Deposits" (2000) University of Southern California.

[38] FEMA 356. "Prestandard and Commentary for the Seismic Rehabilitation of Buildings" (2000) Federal Emergency Management Agency.

[39] Tehrani, M.H., and P.S. Harvey Jr. "Generation of Synthetic Accelerograms for Telecommunications Equipment: Fragility Assessment of a Rolling Isolation System." Bulletin of Earthquake Engineering (2018): doi: 10.1007/s10518-018-0505-7.